

Synthesis and Characterization of New Copper-Chromium Layered Double Hydroxides Pillared with Polyoxovanadates

C. Depège, L. Bigey, C. Forano, A. de Roy, and J. P. Besse¹

Laboratoire de Physico-Chimie des Matériaux, URA CNRS 444, Université Blaise Pascal, Avenue des Landais, 63177 Aubière Cedex, France

Received July 22, 1996; accepted July 24, 1996

In this study, we have focused on the intercalation by ion-exchange of some polyoxovanadate anions from aqueous solution (decavanadate $V_{10}O_{28}^{6-}$, tetravanadate $V_4O_{12}^{4-}$, and pyrovanadate $V_2O_7^{4-}$) into the layers of a copper chromium hydroxalcite-like compound. PXRD, FTIR, TGA, and EXAFS studies have provided information about the specific oxovanadate ions in the interlayers and their orientation. Thermal treatment of these LDHs was also examined. A grafting process of pyrovanadate anions onto the hydroxylated sheets has been demonstrated at room temperature. © 1996 Academic Press, Inc.

INTRODUCTION

The class of materials discussed in this paper are the layered double hydroxides (LDHs), resembling the naturally occurring hydroxalcites (1). These can be represented by the formula $[M_{1-x}^{II}M_x^{III}(\text{OH})_2]^{x+}[A_{x/m}^{m-} \cdot n\text{H}_2\text{O}]^{x-}$, where M^{II} and M^{III} represent metallic cations such as Mg^{2+} , Zn^{2+} , Cu^{2+} , Ni^{2+} and Al^{3+} , Cr^{3+} , Fe^{3+} , respectively (2). In order to avoid the repetition of such heavy formulas, we shall use an abbreviated notation $[M^{II}-M^{III}-A]$.

Structurally, these compounds can be described as positively charged layers of $M(\text{OH})_6$ edge-sharing octahedra, with the interlamellar space being occupied by neutralizing A^{m-} anions and water. One of the most important properties of LDHs is that these interlamellar species can be readily ion exchanged. Various inorganic and organic anions have been intercalated in LDHs, so much is known about the properties of these materials (3–6). Of interest to this study is the intercalation of polyoxometalate ions in hydroxalcite-like compounds (7–23). Polyoxometalates should be ideal pillaring agents for LDHs. These anions generally possess structures consisting of multiple layers of space-filling oxygens and display a wide range of charge densities (24–25). Robust polyoxometalates should impart large gallery heights, and those with suitably high charge

densities should give rise to large anion spacings, thereby providing access to the intracrystalline gallery surfaces.

In this paper, we focus on vanadate ions. Numerous studies have been reported in the literature concerning the intercalation of polyoxovanadate species in LDHs. This intercalation can be made via four different methods: by using an organic precursor (mainly terephthalate one) (8, 13, 14, 18), by exchange without any preswelling agent (19, 20), via calcined precursors directly exposed to a solution of the pillaring species (10, 18, 19), or by direct coprecipitation (21, 22). Recently, a new *chimie douce* method has also been developed by K. S. Han (23) consisting of the insertion of vanadate species directly during the reduction of mixed nickel–cobalt γ -oxyhydroxides in a $\text{NH}_4\text{VO}_3/\text{H}_2\text{O}_2$ medium.

The choice of a layered double hydroxide phase containing copper and chromium metals has been made on the basis of two facts: these phases have not been well-studied (26–28) and, on the other hand, the presence of copper should induce interesting pillaring properties as in copper basic salts (29). Moreover, these polyoxometalate-pillared phases are very useful as catalysts. Indeed, they display high selectivity (near 100%) in the reaction of formation of glycol ethers from ethylene oxide and butanol. Glycol ethers are an important class of chemicals and find applications in paint and ink formulations, jet anti-icing fluids, and brake fluids, so their production in high yield and selectivity is a desirable target. These interesting results will be soon patented in collaboration with BP Chemicals within a Brite-Euram program.

So, this paper concerns the intercalation of three different polyoxovanadate anions in a [Cu–Cr] matrix: the decavanadate $V_{10}O_{28}^{6-}$, the tetravanadate $V_4O_{12}^{4-}$, and the pyrovanadate $V_2O_7^{4-}$. The structure of these species is described in Fig. 1.

The approach taken in synthesizing these materials has been to prepare an organic anion pillared clay precursor (terephthalate or dodecylsulfate) that is subsequently exchanged with the appropriate isopolymetalate under con-

¹ To whom all correspondence should be addressed.

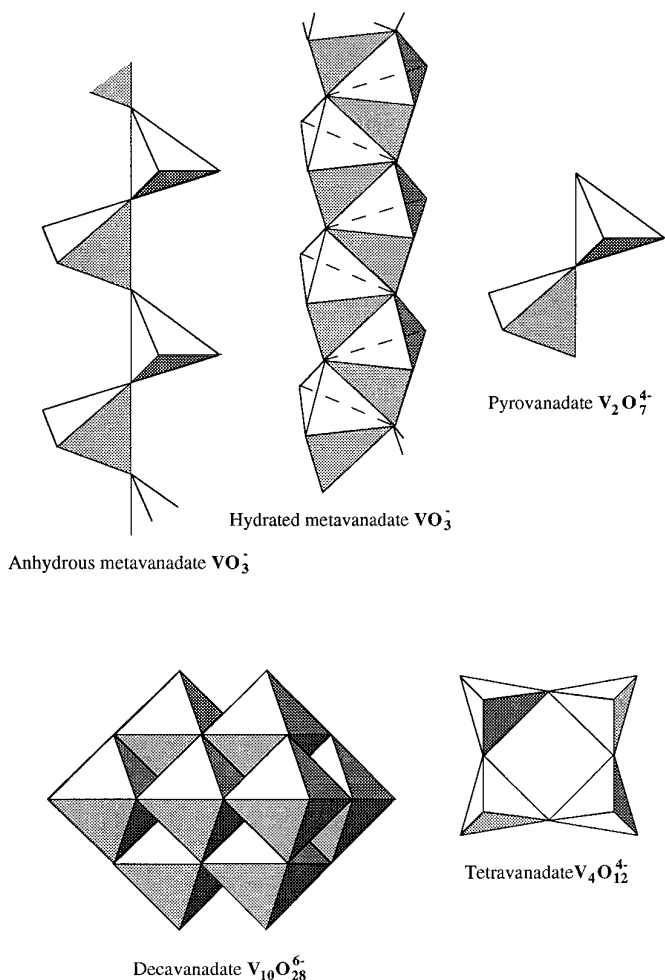


FIG. 1. Structure of some polyoxovanadate species.

trolled pH conditions. Here, the brucite layers are widely separated by the large organic anions prior to isopolymetallate exchange. This approach will be discussed in comparison with the exchange from chloride containing hydroxalcalite.

EXPERIMENTAL

Materials

Analytical reagent grade chemicals were used for all preparations described in this work: $\text{Cu}(\text{NO}_3)_2 \cdot 3\text{H}_2\text{O}$, $\text{CrCl}_3 \cdot 6\text{H}_2\text{O}$, $p\text{-C}_6\text{H}_4(\text{COONa})_2$, $\text{CH}_3-(\text{CH}_2)_{11}-\text{OSO}_3\text{Na}$, NaVO_3 , KCl , and NaOH pellets. All water used was deionized and decarbonated in order to avoid the contamination of our samples by carbonate anions.

Instruments

Powder X-ray diffraction (PXRD) patterns were obtained with a SIEMENS D501 X-ray diffractometer using

$\text{CuK}\alpha$ radiation and fitted with a graphite backend monochromator. Fourier transformed infrared (FTIR) spectra were recorded on pressed KBr pellets with a Perkin–Elmer 16PC spectrophotometer. Thermogravimetric analyses (TGA) were performed with a Setaram TG-DTA92 thermogravimetric analyzer at a typical rate of $5^\circ\text{C}/\text{min}$ under air atmosphere. BET (N_2 at 77 K) surface areas were determined on a Sorptomatic 1900 (Fisons Instruments). Chemical analyses (Cu, Cr, V, Cl, C, S, H, Na) were performed in the Vernaison Analysis Center of CNRS. X-ray adsorption spectra at the K edge of vanadium were obtained at the French L.U.R.E. synchrotron radiation facility. The EXAFS spectrometer was equipped with a Si (311) monochromator. The EXAFS analyses were carried out with programs written by Dr. A. Michalowicz, L.U.R.E. (30).

Synthesis

The synthesis of LDHs is usually achieved by addition of the divalent and trivalent metal salts with an alkaline solution, resulting in the precipitation of the desired product (31–35). We have used this method for the preparation of the [Cu–Cr–Cl] precursor.

[Cu–Cr–Cl]. $\text{Cu}(\text{NO}_3)_2 \cdot 3\text{H}_2\text{O}$ aqueous solution (30 ml, 1 M) and $\text{CrCl}_3 \cdot 6\text{H}_2\text{O}$ solution (15 ml, 1 M) (in order to fix a $\text{Cu}^{2+}/\text{Cr}^{3+}$ ratio equal to 2) were added at a constant flow (4 ml/h) in a beaker containing 100 ml of 2 M KCl solution. The [Cu–Cr–Cl] layered double hydroxide was precipitated at a fixed pH of 5.5 by 40 ml of a 2 M NaOH solution added using an automated titrator (the rate of addition is 4 ml/h). The coprecipitation was carried out at room temperature under vigorous magnetic stirring. The addition was completed in 11 h and the mother liquor was aged under the same conditions for 14 h. Three successive washings using 250 ml of freshly deionized water and centrifugation at 4000 rpm were performed. The precipitate was then dried at 30°C under the room relative humidity conditions (50–60% RH) for 24 h. The resulting solid was then ground into powder prior to characterization. Elemental analysis found Cu, 33.30%; Cr, 13.80%; Cl, 8.50%; H, 2.50%; Na, 0.15%. Calculated for $\text{Cu}_{1.97}\text{Cr}(\text{OH})_{5.94}\text{Cl} \cdot 3.46\text{H}_2\text{O}$: Cu, 33.30%; Cr, 13.83%; Cl, 9.43%; H, 3.42%. The water content as determined by thermogravimetric analysis was 16.57%. X-ray d spacings were 7.70, 3.85, and 2.63 Å.

The syntheses of the other phases (containing polyoxovanadates or organic anions) were carried out with the anionic exchange method (36, 37). Practically, the LDH precursor was suspended in an aqueous solution containing a large excess of the anion to be exchanged at a pH that was in the limits of both LDH and anion stabilities.

[Cu–Cr–TPH] (TPH = Terephthalate dianion). A slurry of 1 g of freshly prepared $\text{Cu}_2\text{Cr}(\text{OH})_6\text{Cl}$ in 50 ml of distilled, carbonate-free water was stirred for 15 min to

ensure complete wetness of the LDH. This slurry was added dropwise to a solution (pH 7.5) containing 50 ml of $p\text{-C}_6\text{H}_4(\text{COONa})_2$ 0.1 M solution. The reaction mixture was stirred for 5 h at room temperature and then the green precipitate was recovered by filtration, washed with three 100 ml portions of deionized water, and dried in air overnight. Its X-ray diffraction pattern, TGA, infrared spectrum, and elemental analysis indicated that the desired product had been obtained. Analysis found Cu, 27.50%; Cr, 11.70%; C, 11.50%; H, 3.70%. Calculated for $\text{Cu}_2\text{Cr}(\text{OH})_6(\text{TPH})_{0.5}$: Cu, 28.50%; Cr, 11.60%; C, 10.80%; H, 3.90%. X-ray d spacing was 13.95 Å. An exchange rate of 100% was obtained.

[Cu–Cr–DDS] (DDS = Dodecylsulfate anion). The method used was the same as that used for [Cu–Cr–TPH], excepted for the pH which was fixed here at the value of 8.5. The product was obtained with an exchange rate of 98%. Analysis found Cu, 19.60%; Cr, 8.40%; C, 25.40%; S, 5.10%; Cl, 0.12%; H, 6.60%. Calculated for $\text{Cu}_2\text{Cr}(\text{OH})_6(\text{DDS})$: Cu, 20.80%; Cr, 8.50%; C, 23.60%; S, 5.20%; H, 6.20%. X-ray d spacing was 25.75 Å.

[Cu–Cr– $\text{V}_{10}\text{O}_{28}$]. Samples of 0.5 g of [Cu–Cr–Cl], [Cu–Cr–TPH], or [Cu–Cr–DDS] LDH powders and 0.8 g of NaVO_3 were added to 50 ml of deionized water at room temperature. The mixture was stirred for 10–15 min before the addition of 2 M HNO_3 dropwise with vigorous stirring (acid was added until the pH dropped to 4.5). Acidification of the LDH phase in the presence of NaVO_3 results in the oligomerization of the metavanadate anion to form the decavanadate anion. The pH was maintained at 4.5 for 5 h. The products were then filtered and washed thoroughly with decarbonated water. The resulting products were allowed to dry in air for 24 h. Elemental analyses and the nature of the obtained phases will be discussed in the following section.

[Cu–Cr– V_4O_{12}]. The procedure used was the same as that used for the decavanadate phase (the three precursors have been tested) with a pH maintained at a value of 7.0 with 2 M HNO_3 .

[Cu–Cr– V_2O_7]. This phase was synthesized as before at a pH value of 10.0 maintained by the addition of 2 M NaOH.

RESULTS AND DISCUSSION

The aqueous chemistry of vanadate ions has been thoroughly examined (24, 25, 38–41). The distribution of ions depends on the concentration and pH. In basic solutions (pH > 9), $\text{V}_2\text{O}_7^{4-}$ is the primary species at a concentration of 0.1 M. Acidification of these species leads to the formation of the $\text{V}_4\text{O}_{12}^{4-}$ ion in the pH range 6–8 and of the $\text{V}_{10}\text{O}_{28}^{6-}$ ion in the pH range 4–6 according to the following equilibria:

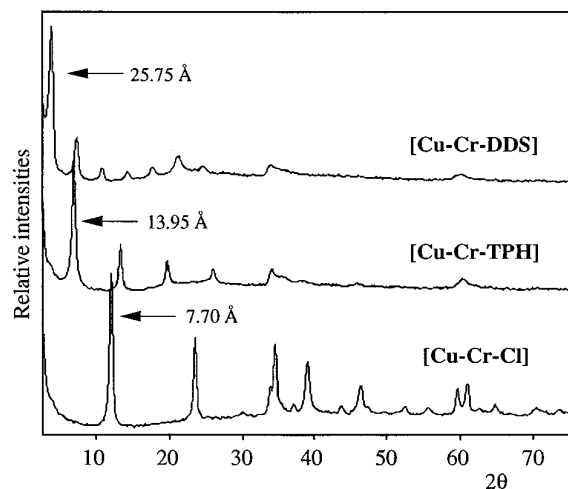
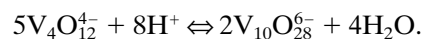
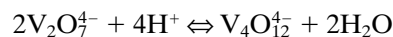


FIG. 2. Powder X-ray diffraction patterns and d spacings of the three different precursors [Cu–Cr–Cl], [Cu–Cr–TPH], and [Cu–Cr–DDS].



These three vanadate ions form the focus of this study.

First, our synthesis strategy consisted of preparing three different pure and well-crystallized precursors as confirmed by X-ray diffraction (Fig. 2). These phases have then been exchanged with a NaVO_3 solution at acid, neutral, or basic pH.

XRD Analysis and Infrared Spectroscopy

Exchange at pH 4.5. In the case of the exchange of [Cu–Cr–TPH] and [Cu–Cr–DDS] precursors (Fig. 3), the

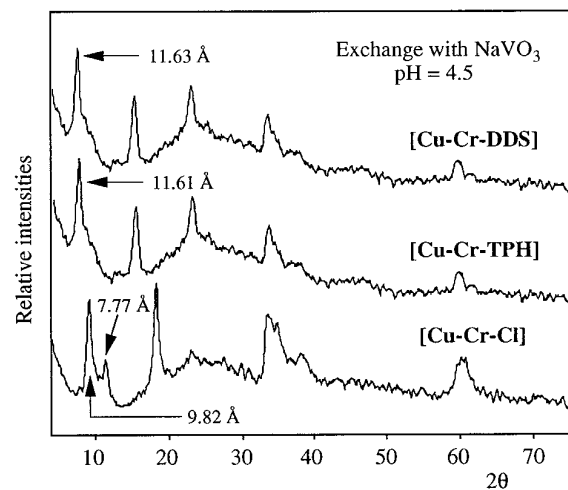


FIG. 3. Powder X-ray diffraction patterns and d spacings of [Cu–Cr–Cl], [Cu–Cr–TPH], and [Cu–Cr–DDS] LDHs exchanged with 0.1 M vanadate solution at pH 4.5.

observed interlamellar distance of 11.6 Å indicates the presence of intercalated decavanadate. Indeed, this poly-oxoanion has already been intercalated in various LDHs. Kwon *et al.* (7) have successfully and totally exchanged decavanadate ions in [Zn–Al–Cl], [Zn–Cr–Cl], and [Ni–Al–Cl] LDHs. The *d* spacing observed is then 11.9 Å. Chibwe and Jones (10) have intercalated this species by reconstruction on a calcined [Mg–Al–CO₃] phase. Even for compounds with a low crystallinity, they noted a *d* spacing not less than 11.8 Å. The slightly shorter distances observed here arise from the presence of strong interactions between the hydroxylated sheets and the V₁₀O₂₈⁶⁻ anion, lying flat in the interlayer domains and pointing the two sets of apical oxygens toward the hydroxylated sheets. With such a disposition, the basal spacing is compatible with the anion height of 7.8 Å. Moreover, this structural hypothesis is confirmed by the absence of any significant contraction under moderate heating. Under calcination at 100°C, the compound retains a relatively high *d* spacing of 11.1 Å, in contrast to other oxoanion containing LDHs.

In the case of the exchange on [Cu–Cr–Cl] precursor (Fig. 3), a different intercalated compound together with the starting chloride product is obtained. The *d* spacing of 9.82 Å seems to be too short compared to the usually observed distance generated by intercalated V₁₀O₂₈⁶⁻ species, as already discussed. This shorter distance should be allocated to the presence of other vanadate species such as the polymerized (VO₃)_{*n*}, as proposed by Ulibarri (18) or more obviously the tetravanadate V₄O₁₂⁴⁻, a hypothesis that is confirmed by infrared and EXAFS studies (Table 2).

Infrared spectra (Fig. 4) confirm the total exchange of the organic anions with the presence of the three characteristic vibration bands of V₁₀O₂₈⁶⁻ species at 954, 814, and 750 cm⁻¹ (Table 2) identified from the sodium decavanadate reference material. These three bands are associated with the vibrations of the VO₆ octahedra (17). Intercalation does not affect the lattice vibrations of the host structure (550 and 450 cm⁻¹). The more complicated spectral feature seen on spectrum b is associated with the presence of V₄O₁₂⁴⁻ anions.

Exchange at pH 7.0. LDH phases obtained at this exchange pH display relatively similar powder X-ray diffractograms (Fig. 5) to the ones prepared at more acidic pH. The main changes concern slight shifts in distances and strong modifications in relative intensities. Two different intercalation modes are evidenced, leading to a high-basal-spacing phase (either *d* = 10.38 or 12.10 Å, depending on the nature of the organic anion to be replaced) and a phase with a low interlayer distance (9.62 Å). Identification of the already mentioned vanadate species is confirmed by infrared spectroscopy.

In Fig. 6, clear evidence is demonstrated that spectra a and c are, respectively, characteristic of pure intercalated

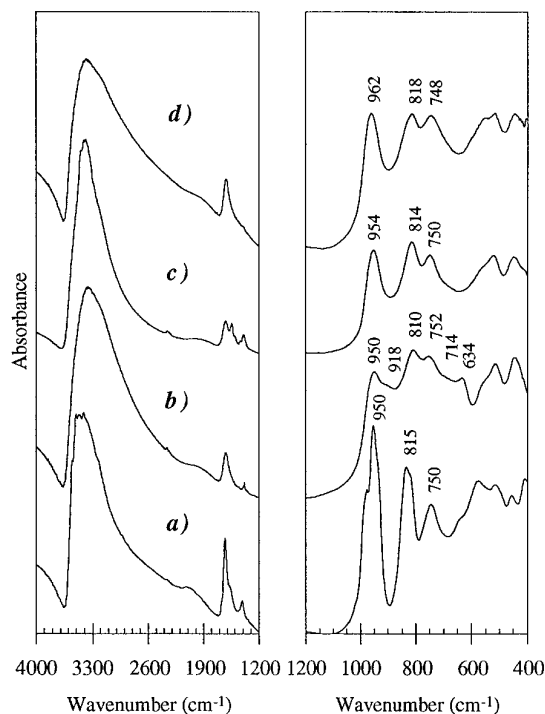


FIG. 4. Infrared spectra of (a) Na₆V₁₀O₂₈ · 18H₂O and of (b) [Cu–Cr–Cl], (c) [Cu–Cr–TPH], and (d) [Cu–Cr–DDS] exchanged with 0.1 M vanadate solution at pH 4.5.

V₄O₁₂⁴⁻ and V₁₀O₂₈⁶⁻ isopolyanions. Spectrum b arises obviously from the contribution of both species, indicating that the prepared phase is not pure. These results give the first example of an intercalation of pure tetravanadate in LDH. Even if a minor chloride LDH phase is detected on the

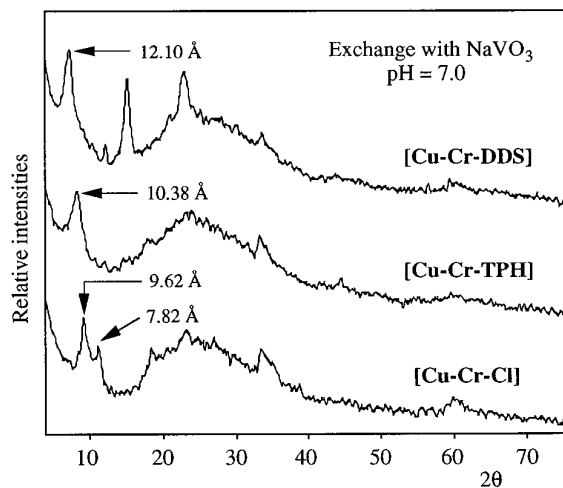


FIG. 5. Powder X-ray diffraction patterns and *d* spacings of [Cu–Cr–Cl], [Cu–Cr–TPH], and [Cu–Cr–DDS] LDHs exchanged with 0.1 M vanadate solution at pH 7.0.

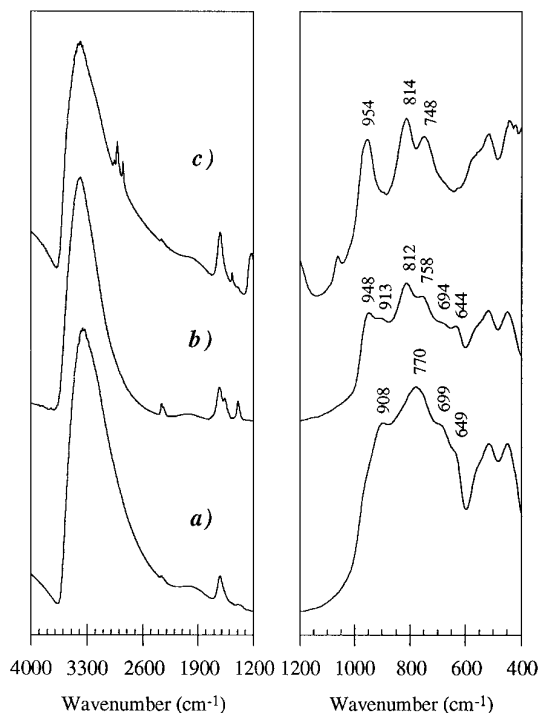
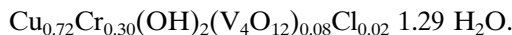


FIG. 6. Infrared spectra of (a) [Cu-Cr-Cl], (b) [Cu-Cr-TPH], and (c) [Cu-Cr-DDS] exchanged with 0.1 *M* vanadate solution at pH 7.0.

diffraction pattern, elemental analysis (Table 1) confirms the exchange. We can then propose the corresponding chemical formula

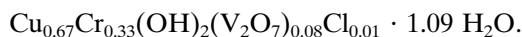


The infrared spectrum of this phase is characteristic of VO_4 tetrahedra ($\nu_s(\text{OVO})$ at 920 cm^{-1}) with tetrahedra linkage ($\nu_s(\text{VOV})$ at 660 cm^{-1}).

Exchange at pH 10.0. At this value of pH, no exchange is obtained from [Cu-Cr-DDS] LDH as is shown in Fig. 7. Incomplete exchange was already obtained at pH 7.0 with this precursor as shown on the infrared spectrum in the C-H vibrations region (Fig. 6). On the other hand, the similitude between the infrared spectra of [Cu-Cr-TPH] exchanged at pH 10 (Fig. 8) and [Cu-Cr-Cl] exchanged at pH 7.0 shows in both compounds the presence of pyrovanadate anions or condensed VO_4 tetrahedra in the interlamellar domains.

The phase prepared from the chloride precursor displays the best crystallinity even though an amorphous compound is present in a minor amount. The short interlayer distance can be better accounted for by the intercalation of the smaller vanadate anion $\text{V}_2\text{O}_7^{4-}$. The presence of $\text{V}_2\text{O}_7^{4-}$ species is also demonstrated by both IR with the characteristic VO_4 bands at 858, 784, and 704 cm^{-1} (Table 2) and

elemental analysis (Table 1), which allows one to conclude in favor of the formula



The short interlamellar distance observed (7.62 \AA) is not compatible with free intercalated oxoanions at hydrogen bond distances from hydroxyl planes on either sides; such disposition usually generates basal-plane spacing not lower than 8.9 \AA .

This observation should be better explained by a grafting of the V_2O_7 species onto the hydroxylated layers. This contraction process has been observed for other MO_4 or M_2O_7 oxoanions in [Zn-Al], [Zn-Cr], and [Cu-Cr] LDH host structures (28, 42). It can occur either spontaneously during aging or storing, or under moderate thermal treatment ($100\text{--}150^\circ\text{C}$). As an example, comparison can be made with the analogous lamellar alvanite (45) mineral structure $[(\text{Zn}, \text{Ni})\text{Al}_4(\text{OH})_{12}][(\text{VO}_3)_2] \cdot 2\text{H}_2\text{O}$ built from a stacking of bayerite-like hydroxylated layers $[(\text{Zn}, \text{Ni})\text{Al}_4(\text{OH})_{12}]$, maintained by interlayered VO_3 single chains. In such a structure, the $\text{V}_2\text{O}_7^{4-}$ ditetrahedron entity is strongly hydrogen bonded (Fig. 9) to the OH planes, and this bonding leads to a high basal-plane spacing of 8.9 \AA . In the prepared [Cu-Cr- V_2O_7] LDH, the $\text{V}_2\text{O}_7^{4-}$ anion is probably directly bound to the Cu^{2+} and Cr^{3+} cations of the layers. This grafting occurs through the replacement of two adjacent OH groups of one OH layer by two oxygen atoms of the ditetrahedra (Fig. 10) as has been proposed for the [Cu-Cr- Cr_2O_7] LDH phase (28).

We must notice that the hypothesis of a pillaring of the layers to a three-dimensional reticulated phase must be ruled out from the point of view of interlayer distance while such pillaring can be depicted in the synthetic volborthite $\text{Cu}_3\text{V}_2\text{O}_7(\text{OH})_2 \cdot 2\text{H}_2\text{O}$ (46). Its structure is constituted of lacunar brucite-like layers of the formula $\square M_3X_8$ (copper atoms occupying three-fourths of the octahedral sites) linked to each other by pyrovanadate groups (Fig. 11). The interlamellar distance observed (7.21 \AA) is much shorter than that of the pyrovanadate LDH phase, indicating that a different grafting process occurs. The same distance was observed by K. S. Han (23) after a thermal treatment at 190°C of a $[\text{Ni-Co}-(\text{VO}_3)_n^-]$ LDH (Fig. 12). The interlamellar distance decreases from 9.15 \AA before thermal treatment (corresponding to $(\text{VO}_3)_n^-$ metavanadate anionic chains intercalated within the interslab space) to 7.21 \AA . This short distance is due to a grafting of the VO_4 tetrahedra to two adjacent slabs coupled with a partial chain fragmentation and a removal of water.

DISCUSSION

In Table 3 are listed the different LDH phases obtained from exchange on the three precursors at the three differ-

TABLE 1
Elemental Analysis of the Phases Obtained by Exchange of the Three Precursors with 0.1 M Vanadate Solution at pH 4.5, 7.0, and 10.0

Anionic species		$V_{10}O_{28}^{6-}$			$V_4O_{12}^{4-}$	$V_2O_4^{2-}$
		[Cu-Cr-Cl]	[Cu-Cr-TPH]	[Cu-Cr-DDS]	[Cu-Cr-Cl]	[Cu-Cr-Cl]
Cu	Exp.	27.1	24.1	20.7	30.2	32.4
	Calc.	26.0	24.4	24.4	27.8	32.3
Cr	Exp.	11.7	9.7	9.4	10.4	13.2
	Calc.	10.6	10.0	10.0	11.3	13.2
V	Exp.	14.2	16.0	18.5	10.8	6.3
	Calc.	17.4	16.3	16.3	11.1	6.4
H	Exp.	2.3	2.4	2.6	2.6	2.5
	Calc.	2.3	2.8	2.8	3.2	3.2
C	Exp.	—	1.8	2.9	—	—
	Calc.	—	0	0	—	—
S	Exp.	—	—	0.5	—	—
	Calc.	—	—	0	—	—
Cl	Exp.	0.4	—	—	0.46	0.18
	Calc.	0	—	—	0	0
$x = \frac{Cr^{3+}}{Cu^{2+} + Cr^{3+}}$	Exp.	0.345	0.330	0.357	0.294	0.332
	Calc.	0.333	0.333	0.333	0.333	0.333
Exchange rate (%)		94	93	84	94	98

ent pH tested. The main conclusions drawn from this preparative study point out the effect of the nature of the anions to be exchanged and the pH of exchange on the selective intercalation of the various vanadate species. It appears clearly that the size of the precursor anion and more fundamentally the values of the interlayer distances must favor the intercalation of vanadate of similar hinder-

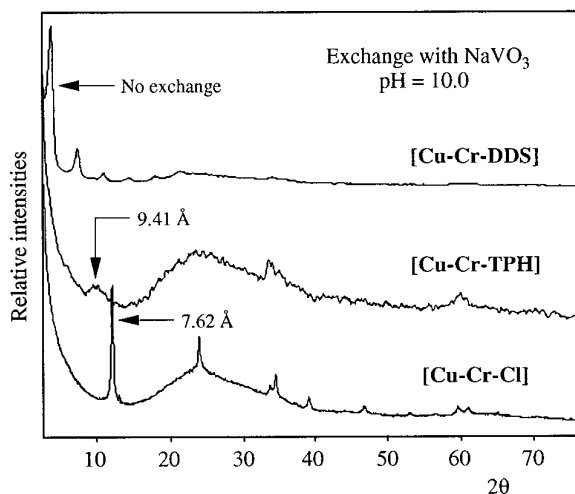


FIG. 7. Powder X-ray diffraction patterns and d spacings of [Cu-Cr-Cl], [Cu-Cr-TPH], and [Cu-Cr-DDS] LDHs exchanged with 0.1 M vanadate solution at pH 10.0.

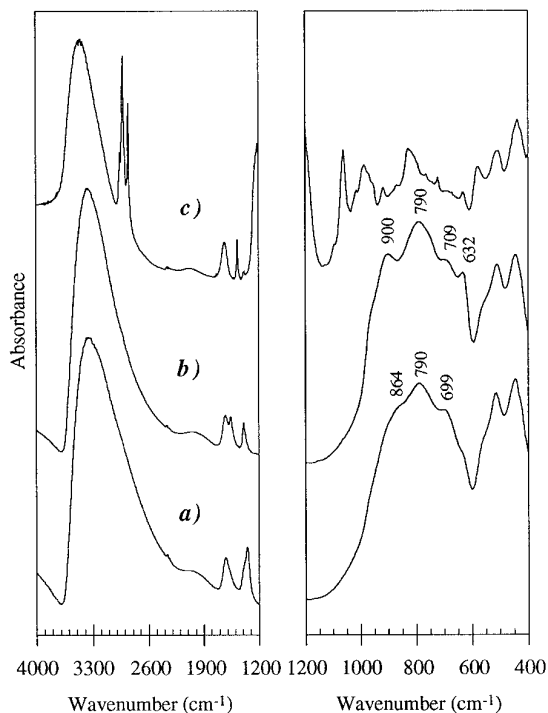


FIG. 8. Infrared spectra of (a) [Cu-Cr-Cl], (b) [Cu-Cr-TPH], and (c) [Cu-Cr-DDS] exchanged with 0.1 M vanadate solution at pH 10.0.

TABLE 2
Infrared Identification of the Different Phases Obtained after Exchange with 0.1 M Vanadate Solution on [Cu–Cr–Cl], [Cu–Cr–TPH], and [Cu–Cr–DDS] LDHs Compared with Previously Published Results

Precursor	pH	Isopolyanions vibration bands (cm ⁻¹)					
		$\nu(\text{VO}_2)$ sym	$\nu(\text{VO}_2)$ sym	$\nu(\text{VO}_2)$ asym	$\nu(\text{VOV})$ asym	$\nu(\text{VOV})$ sym	
[Cu–Cr–Cl] [Cu–Cr–TPH] [Cu–Cr–DDS] $\text{V}_{10}\text{O}_{28}^{6-}$ (43)	4.5	950	918	810	752	714	634
[Cu–Cr–Cl] [Cu–Cr–TPH] [Cu–Cr–DDS] $\text{V}_4\text{O}_{12}^{4-}$ (23)	7.0	948	913	812	758	694	644
[Cu–Cr–Cl] [Cu–Cr–TPH] [Cu–Cr–DDS] $\text{V}_2\text{O}_4^{2-}$ (44)	10.0	—	864	790	—	699	632
			900	790	—	709	632
			—	—	—	710	—

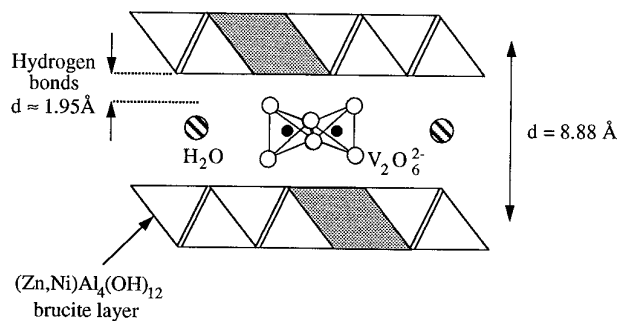


FIG. 9. Structure of alvanite $(\text{Zn,Ni})\text{Al}_4(\text{OH})_{12}(\text{V}_2\text{O}_6) \cdot 2\text{H}_2\text{O}$.

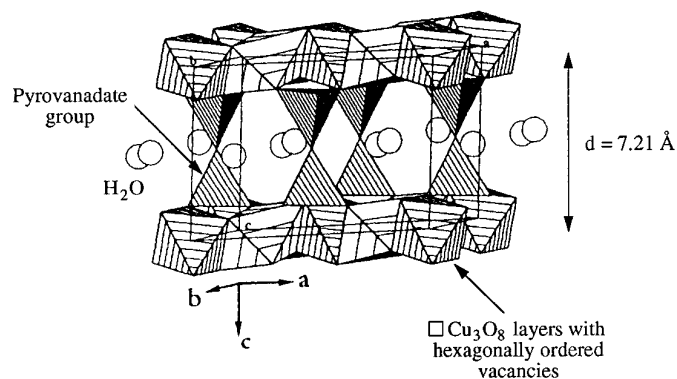


FIG. 11. Structure of volborthite $\text{Cu}_3\text{V}_2\text{O}_7(\text{OH})_2 \cdot 2\text{H}_2\text{O}$.

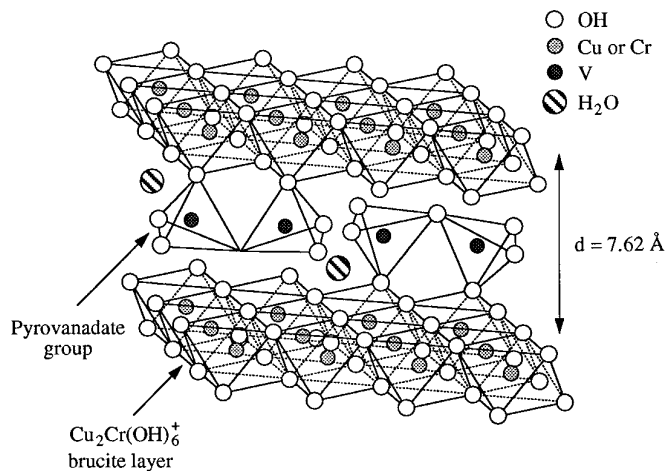


FIG. 10. Schematic representation of grafting process of $\text{V}_2\text{O}_4^{2-}$ species onto $\text{Cu}_2\text{Cr}(\text{OH})_6^+$ brucitic sheets.

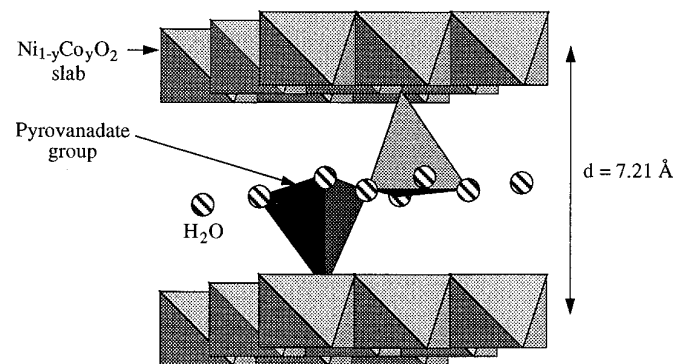


FIG. 12. Schematic representation of grafting process of $(\text{VO}_3)_n^-$ metavanadate chains onto $\text{Ni}_2\text{Co}(\text{OH})_6$ slabs after a thermal treatment at 190°C .

TABLE 3
 Identification by Powder X-Ray Diffraction and Infrared Spectroscopy of the Different Phases Obtained after Exchange with 0.1 M Vanadate Solution on [Cu–Cr–Cl], [Cu–Cr–TPH], and [Cu–Cr–DDS] Precursors

Exchange with	Precursor	d (Å)	Phases (identification by PXRD/FTIR)
NaVO ₃ pH 4.5	[Cu–Cr–Cl]	9.82	[Cu–Cr–V ₁₀ O ₂₈] or [Cu–Cr–(VO ₃) _{<i>n</i>}]
		7.77	[Cu–Cr–Cl]
	[Cu–Cr–TPH]	11.62	[Cu–Cr–V ₁₀ O ₂₈]
	[Cu–Cr–DDS]	11.63	[Cu–Cr–V ₁₀ O ₂₈]
NaVO ₃ pH 7.0	[Cu–Cr–Cl]	9.62	[Cu–Cr–V ₄ O ₁₂]
		7.82	[Cu–Cr–Cl]
	[Cu–Cr–TPH]	10.38	[Cu–Cr–V ₄ O ₁₂]
	[Cu–Cr–DDS]	12.10	[Cu–Cr–V ₁₀ O ₂₈]
NaVO ₃ pH 10.0	[Cu–Cr–Cl]	7.62	[Cu–Cr–V ₂ O ₇]
	[Cu–Cr–TPH]	9.41	[Cu–Cr–V ₄ O ₁₂]
	[Cu–Cr–DDS]	—	No exchange

ence. This is particularly true for the chloride precursor, which cannot directly exchange the voluminous V₁₀O₂₈⁶⁻ anion. Exchange using a swelling agent such as glycerol has been demonstrated to be successful for this purpose. The pH value seems also to play a role in the exchange reaction, in particular when using the [Cu–Cr–DDS] LDH precursor. It not only determines the nature of the vanadate species in equilibrium in the solution, but its value also seems to affect the exchange rate. For the dodecylsulfate anion, the solvation properties of the anionic surfactant are probably not compatible with a basic medium and they prevent any replacement from the LDH structure.

EXAFS Study

A complementary EXAFS study at the K edge of vanadium allows us to confirm the nature of the intercalated species. Figure 13a shows the Fourier transformed EXAFS spectra of pure [Cu–Cr–V₁₀O₂₈] (synthesized from terephthalate precursor) and of the Na₆V₁₀O₂₈ · 18H₂O, compound of well-known structure with vanadium atoms in octahedral sites. The spectra are relatively similar with only small distance shifts and intensity variations, probably due to a certain distortion of the polyoxometalate between the sheets. The three maxima of radial electron density are easily assigned to the three first shells arising from, respectively, oxygen atoms for the first and third peaks and vanadium atoms for the second peak. The Fourier transformed EXAFS spectra of [Cu–Cr–V₂O₇] and [Cu–Cr–V₄O₁₂] LDHs are plotted in Fig. 13b. The single-peak spectra observed for these samples are characteristic of a vanadium

tetrahedral environment of low condensed vanadate species.

Thermogravimetric Analysis and Surface Area Measurements

The TGA patterns of [Cu–Cr–V₁₀O₂₈], [Cu–Cr–V₄O₁₂], and [Cu–Cr–V₂O₇] LDHs are shown in Fig. 14. All phases lose adsorbed and intercalated water molecules below 200°C. Relative contents of both H₂O types vary from one phase to the other depending on their interlayer accessibility and their surface properties. The dehydroxylation of the brucite-like sheets occurs between 200 and 400°C. The shift of the dehydroxylation starting temperature indicates a slight thermal stabilizing effect of the pyrovanadate and tetravanadate anions on the bulk layers. Above 400°C, decomposition of the vanadate species occurs giving rise to various vanadium oxides.

The specific surface area of the decavanadate and pyrovanadate LDH phases calcined at 200°C for 18 h under vacuum are low, respectively 42 and 70 m²/g. Heating the products at 400°C under the same conditions resulted in a decrease in the surface areas, which drop, respectively, to 21 and 30 m²/g. Although isopolymetalate-pillared hydrotalcites lose significant amounts of water upon calcination, the resulting products show little variation in surface area. By construction of idealized models of these materials, Drezdron (8) has shown that the space between adjacent isopolymetalate pillars is barely large enough for interlayer water molecules. Assuming that the pillars are less than ideally distributed, especially after calcination, voids

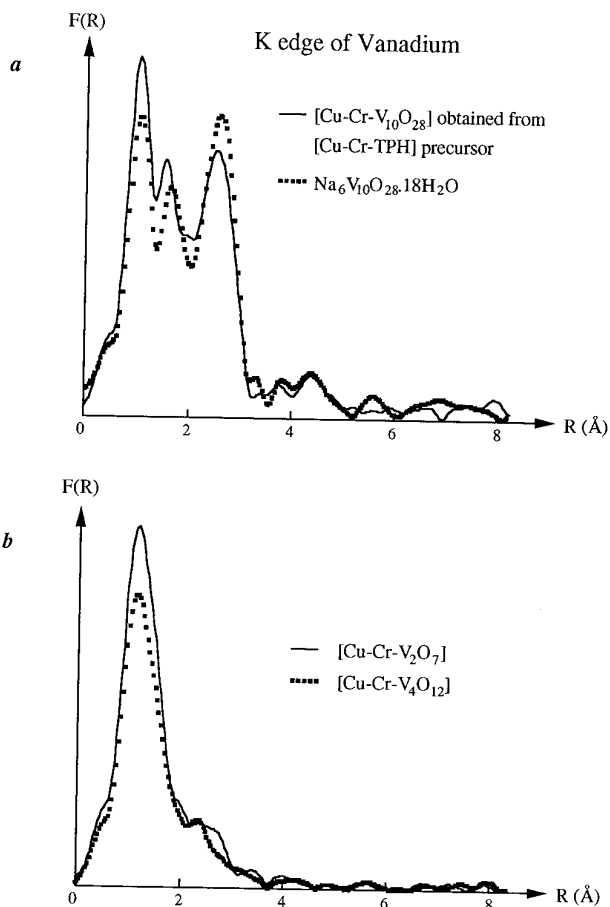


FIG. 13. Fourier transformed EXAFS spectra at the K edge of vanadium of (a) $\text{Na}_6\text{V}_{10}\text{O}_{28} \cdot 18\text{H}_2\text{O}$ and $[\text{Cu-Cr-V}_{10}\text{O}_{28}]$ synthesized from the terephthalate precursor (vanadium in octahedral sites) and of (b) $[\text{Cu-Cr-V}_2\text{O}_7]$ and $[\text{Cu-Cr-V}_4\text{O}_{12}]$.

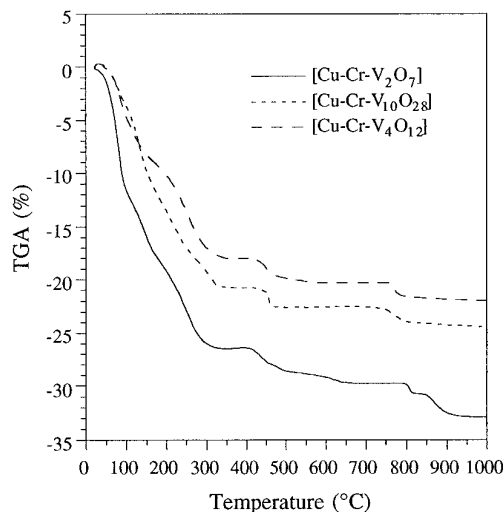


FIG. 14. TGA curves of $[\text{Cu-Cr-V}_2\text{O}_7]$, $[\text{Cu-Cr-V}_{10}\text{O}_{28}]$, and $[\text{Cu-Cr-V}_4\text{O}_{12}]$ LDHs under air atmosphere.

in the interlayer domain may be difficult if not impossible to access due to pore blockage. This hypothesis should be extended to the pyrovanadate phase.

CONCLUSION

The major conclusions of the different points examined in this study are as follows:

— Ion exchange of polyoxovanadate anions in $[\text{Cu}_2\text{Cr}(\text{OH})_6]^+$ sheets from an aqueous solution is influenced by pH. At pH 10–11, $\text{V}_2\text{O}_7^{4-}$ is selectively ion-exchanged, whereas as the pH is dropped, the major interlayer species are $\text{V}_4\text{O}_{12}^{4-}$ (pH 6–7) and $\text{V}_{10}\text{O}_{28}^{6-}$ (pH 4–5).

— The intercalation of pyrovanadate species induces an immediate grafting process, even without any thermal treatment.

— All phases display relatively low values of specific surface areas (around $30 \text{ m}^2/\text{g}$).

— The catalytic activity of these materials has been demonstrated in etherification reactions.

ACKNOWLEDGMENT

We are grateful to the European Community which supports this work, realized under a Brite-Euram program.

REFERENCES

1. R. Allmann, *Acta Crystallogr. B* **24**, 972 (1968).
2. S. Miyata and A. Okada, *Clays Clay Miner.* **25**, 14 (1977).
3. A. Schutz and P. Biloën, *J. Solid State Chem.* **68**, 360 (1987).
4. H. Boehm, J. Steinle, and C. Vieweger, *Angew. Chem., Int. Ed. Engl.* **16**, 265 (1977).
5. K. J. Martin and T. J. Pinnavaia, *J. Am. Chem. Soc.* **108**, 541 (1986).
6. M. Meyn, K. Beneke, and G. Lagaly, *Inorg. Chem.* **29**, 5201 (1990).
7. T. Kwon, G. A. Tsigdinos, and T. J. Pinnavaia, *J. Am. Chem. Soc.* **110**, 3653 (1988).
8. M. A. Drezdron, *Inorg. Chem.* **27**, 4628 (1988).
9. T. Kwon and T. J. Pinnavaia, *Chem. Mater.* **1**, 381 (1989).
10. K. Chibwe and W. Jones, *Chem. Mater.* **1**, 489 (1989).
11. M. Doeuff, T. Kwon, and T. J. Pinnavaia, *Synthetic Met.* **34**, 609 (1989).
12. J. Twu and P. K. Dutta, *J. Phys. Chem.* **93**, 7863 (1989).
13. J. Twu and P. K. Dutta, *J. Catal.* **124**, 503 (1990).
14. E. D. Dimotakis and T. J. Pinnavaia, *Inorg. Chem.* **29**, 2393 (1990).
15. J. Twu and P. K. Dutta, *Chem. Mater.* **4**, 398 (1992).
16. J. Wang, Y. Tian, R. C. Wang, and A. Clearfield, *Chem. Mater.* **4**, 1276 (1992).
17. E. Lopez Salinas, and Y. Ono, *Bull. Chem. Soc. Jpn.* **65**, 2465 (1992).
18. M. A. Ulibarri, F. M. Labajos, V. Rives, W. Kagunya, W. Jones, and R. Trujillano, *Mol. Cryst. Liq. Cryst.* **244**, 167 (1994).
19. F. Kooli, V. Rives, and M. A. Ulibarri, *Inorg. Chem.* **34**, 5114 (1995).
20. F. Kooli, V. Rives, and M. A. Ulibarri, *Inorg. Chem.* **34**, 5122 (1995).
21. A. Bhattacharyya, D. B. Hall, and T. J. Barnes, *Appl. Clay Sci.* **10**, 57 (1995).
22. F. Kooli and W. Jones, *Inorg. Chem.* **34**, 6237 (1995).
23. K. S. Han, Ph.D. Thesis, Université Bordeaux I, France, 1996.
24. M. T. Pope, "Heteropoly and Isopoly Oxometalates." Springer-Verlag, New York, 1983.

25. L. Pettersson, B. Hedman, I. Andersson and N. Ingri, *Chem. Scripta*, **22**, 254 (1983).
26. K. El Malki, A. de Roy, and J. P. Besse, *Eur. J. Solid State Inorg. Chem.* **26**, 339 (1989).
27. R. P. Grosso, S. L. Suib, R. S. Weber, and P. F. Schubert, *Chem. Mater.* **4**, 922 (1992).
28. C. Depège, C. Forano, A. de Roy, and J. P. Besse, *Mol. Cryst. Liq. Cryst.* **244**, 161 (1994).
29. S. Yamanaka, T. Sako, K. Seki, and M. Hattori, Proc. of 8th International Conference on Solid State Ionics, Lake Louise, Canada, 1991.
30. A. Michalowicz, Logiciels pour la chimie, Société Française de Chimie, Paris, p. 102–103, 1991.
31. W. T. Reichle, *Solid State Ionics* **22**, 135 (1986).
32. S. Miyata, *Clays Clay Miner.* **23**, 369 (1975).
33. S. Miyata, *Clays Clay Miner.* **28**, 50 (1980).
34. W. T. Reichle, S. Y. Kang, and D. S. Everhardt, *J. Catal.* **101**, 352 (1986).
35. E. Suzuki, S. Idemura, and Y. Ono, *Clays Clay Miner.* **32**, 173 (1989).
36. S. Miyata, *Clays Clay Miner.* **31**, 305 (1983).
37. K. Itaya, C. Hien-Chang, and U. Isamu, *Inorg. Chem.* **26**, 624 (1987).
38. C. S. G. Phillips and R. J. P. Williams, “Inorganic Chemistry,” Oxford, 1965.
39. T. Debaerdemaeker, J. M. Arrieta, and J. M. Amigo, *Acta Crystallogr. B* **38**, 2465 (1982).
40. V. W. Day, W. G. Klemperer, and D. J. Maltbie, *J. Am. Chem. Soc.* **109**, 2991 (1987).
41. P. Comba and L. Helm, *Helvetica Chim. Acta* **71**, 1406 (1988).
42. C. Forano, A. de Roy, C. Depège, M. Khaldi, F. Z. El Metoui, and J. P. Besse, *Am. Chem. Soc.* **40**, 317 (1995).
43. J. Fuchs, S. Mahjour, and R. Palm, *Z. Naturforsch. B* **31**, 544 (1976).
44. K. Nakamoto, “Infrared and Raman Spectra of Inorganic and Coordination Compounds.” Wiley, New York, 1986.
45. F. Pertlik and P. J. Dunn, *N. Jb. Miner. Mh.* **9**, 385 (1990).
46. M. A. Lafontaine, A. Le Bail, and G. Ferey, *J. Solid State Chem.* **85**, 220 (1990).